21st Australasian Fluid Mechanics Conference
Adelaide, Australia
10-13 December 2018

Turbulence Characteristics of a Tidal Embayment

K.A. Suara[1], M. Khanarmuei [1], B.T. Kettle[1] and R.J. Brown[1]

[1]Environmental Fluid Mechanics Research Group,

Queensland University of Technology, Queensland 4000, Australia

Abstract

There is a lack of observations of near-bed turbulence characteristics in hypersaline estuaries with inverse circulation. With the aim of providing baseline flow and turbulence characteristics of such system, a field study was carried out in Hervey Bay, a tidal embayment. The flow field from the bed to the mid-water column was measured using a 2MHz Aquadopp upward-looking acoustic Doppler current profiler (ADCP). The turbulence characteristics of the bottom boundary layer were measured using a downward-looking 5-beam Signature1000 ADCP in high resolution configuration. In order to evaluate the energy budget within the channel, we performed and present a preliminary estimate of the rate of dissipation of turbulent kinetic energy, ε, within the channel. The ε varied up to four orders of magnitude within two diurnal tidal cycles, and ranged between 10^{-6} - 10^{-2} m^2/s^3 for the spring and between 10^{-8} - 10^{-5} m^2/s^3 for the neap tides. These estimates were within the range observed in similar tidal channels.

Introduction

Improvement in instrumentation has enabled measurements of the rate of dissipation of turbulent kinetic energy, ε, which has led to major advances in our understanding of the mechanism of turbulent processes and their parameterisation [5, 11]. Observations of turbulence in large estuarine embayments are of increasing interest for validating numerical models and investigating sediment transports [9]. This need is fuelled by the distinctive turbulent behaviour of estuaries, which is strongly influenced by their varying geomorphological structures and the climatic conditions of their location. There is a lack of observations of near-bed turbulence characteristics in hypersaline estuaries, with inverse circulation, as compared with estuaries with significant freshwater input. To this end, we report on turbulence measurements acquired at Hervey Bay, Queensland, Australia. The measurement location is approximately at the site of the scuttling of ex-HMAS Tobruk, a retired military vessel, for an underwater museum. The field work study was conducted before the scuttling in July, 2018.

Field, experiment and instrumentation

Hervey Bay (Long. 153.805°E, Lat. 24.8842°S) is northward-facing with an 80 km-wide opening to the Great Barrier Reef (GBR) lagoon, with a mean depth of approximately 20 m and a north-south length of around 60 km. The mouth opens northward and it narrows southwards. The climate around the bay is subtropical with no distinct dry period, but with most precipitation occurring during the summer months [2]. The vast area of Hervey Bay is characterised as having inverse circulation which occurs as a result of the extensive shallow parts of the bay, allowing very high rates of evaporation to occur.

In a field study during the summer period, two acoustic Doppler current profilers were deployed in Hervey Bay for 53 days between January 23 and March 20, 2018 covering neap and spring tidal cycles. A three-beam Nortek Aquadopp 2MHz system was deployed in an upward-looking configuration and sampled continuously with measurement intervals of 300 s to provide the mean flow between 0.3 m and 14 m above the sediment water interface. A five-beam Nortek Signature1000 series sampling continuously at 4 Hz was deployed in a downward-looking configuration to provide a detailed high-resolution turbulent measurement at 2.3 m above the bed with a bin size of 0.02 m. The inclusion of a fifth beam in the vertical direction of the Signature1000 series allows for a true measurement of vertical velocities and analysis of the turbulence characteristics with minimal influence of the mean flow.

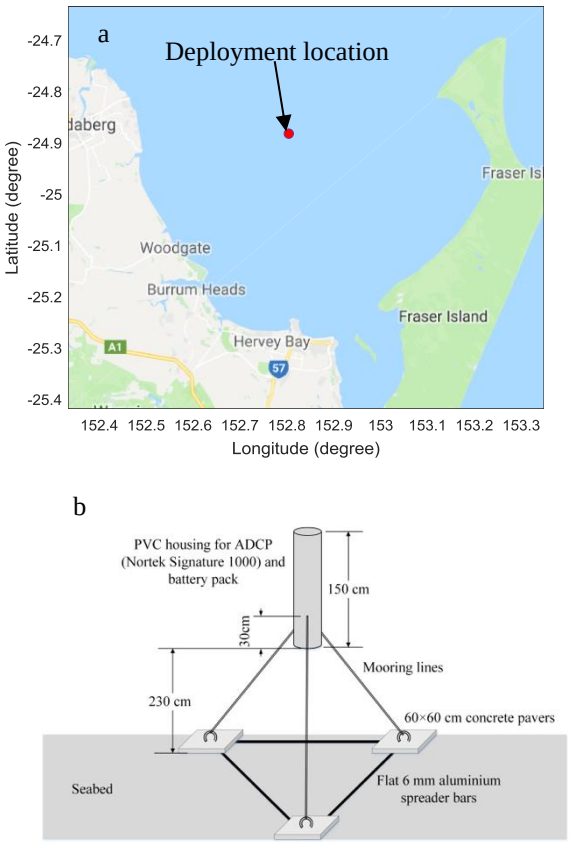

Figure 1. (a) Map of study location, Hervey Bay, (Longitude 153.924◦ E, Latitude 24.8465◦ S) (Google, 2013); (b) Sketch of the downward looking ADCP mount.

The Aquadopp ADCP was deployed with a fixed mount which kept the first beam at 0.3 m above the bed. The Signature1000 series was deployed using a customised trawler-proof mooring configuration. The configuration consisted of a positively buoyant

cylinder with a metacentre designed to be closer to the base where the Signature1000 series and external battery canister was placed for ballasting. The positive buoyancy of the cylinder can cause the instrument to oscillate at the natural frequency of the cylinder. To reduce the amplitude of this oscillation, the configuration was tethered to three anchor weights in equilateral triangular configuration on the bed, and connected to the cylinder at approximately the metacentre as shown in Figure 1b. Furthermore, orientation and motion of the platform were obtained concurrently to correct for bias in turbulence parameter estimates that are sensitive to platform motion. However, estimates of rate of dissipation of turbulent kinetic energy (TKE) from the structure function method used herein have been shown in literature [4] and in the data analysis section not to be significantly contaminated by the mooring motion for the tethered ADCP, therefore motion correction was not implemented.

Data analysis

Quality Control

The raw high frequency beam velocity data might contain some level of noise, spikes, fish movement and low-correlated outputs which are spurious but could be mistaken for physical processes in high-turbulence environmental flows. Herein, beam velocity data are first quality controlled by removing data with correlation less than 50% and echo beam amplitude less than 30dB, as recommended by the manufacturer. This identified only a very small fraction (< 0.1%) of the dataset as spurious. A visual inspection of the vertical velocity dataset from the downward-looking ADCP indicated the presence of spikes which fulfilled the aforementioned criteria. Therefore, for the turbulence analysis presented here, the vertical 5th beam data were further de-spiked using phase-space threshold method [1]. The vertical-beam velocity contained some points with large magnitude which were an artefact of heaving (bobbing) of the platform. These outliers were further removed for the individual bin using a threshold corresponding to two standard deviations of the 48-hour vertical velocity time series. The spurious data and spikes in the dataset were 5 - 10% of the individual 48-hour window. For the analyses presented herein, these data points were not replaced except for spectral analysis, where they were replaced with zeros.

Frequency spectra

Frequency spectra are used to evaluate waves and the mooring motion as well as their effects on the vertical-beam velocities and the structure function. The spectra are estimated with a Hamming window average of 4098-points with 50% overlap along 48-hours observation, resulting in at least 336 degrees of freedom and a frequency resolution of 0.002 Hz. Figure 2a shows the spectra of the orientation data (pitch, roll and heading) and the pressure of the downward-looking ADCP. The spectra all showed broad peaks at frequencies around 0.1 Hz and 0.4 Hz. The peak at 0.1 Hz corresponds to the significant wave frequency within Hervey Bay while 0.4 Hz is approximately the natural frequency of the deployment platform. Similar peaks were found in the spectra of the along-beam velocity of the vertical beam (Figure 2b). This indicates that the wave and mooring motions contaminate the spectra of the vertical velocities. The spectra of the velocity structure function at three length scales, r = 0.1, 0.4 and 1 m are shown in Figure 2b. The results showed that the velocity differences along the beam are less susceptible to contamination from the mooring platform motion. This suggested that the contamination is an offset on the entire along-beam profile and does not significantly affect the structure function. Moreover, the structure function spectra are consistent with the turbulence cascade, with the increase in the energy density with the eddy length scale, r.

Structure function and TKE dissipation rate

The along-beam velocities can be used to estimate the second-order spatial structure which is the mean-square of the velocity fluctuation difference between two points separated by a distance r. Following the method described in [11] and validated in [7], for each z location using the structure function can be defined as:

$$D(z,r_o) = \left\langle \left[(u'(z) - u'(z-r) \right]^2 \right\rangle \quad (1)$$

where u' is the along-beam velocity fluctuation after removing the temporal mean, z is the vertical location from the bottom, r is the distance between bins and the negative sign between z and r is indicating that the structure function is one-sided with the difference taken from top bin downward towards the bed.

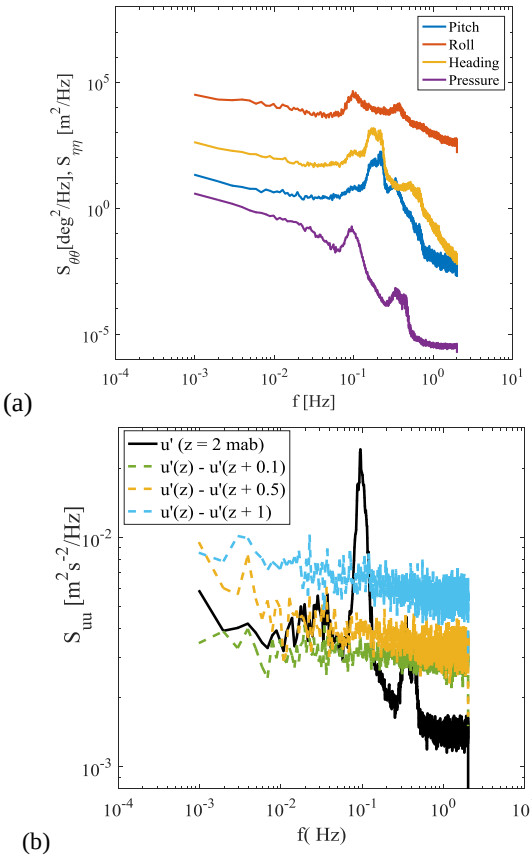

Figure 2. (a) Frequency spectra (a) the orientation data and the pressure (b) vertical-beam velocity and velocity difference: (See text for detailed description)

The mooring motion caused an offset of the bin beam velocities, therefore neighbouring velocity estimates were no longer independent when the instrument bobs and tilts [10]. This bias can be removed by removing the correction factor Δr from the original lag distances, such that $r = r_o - \Delta r$. Following [10] Δr can be estimated as:

$$\Delta r = \left(\frac{\sigma_z}{\cos\bar{\theta}} \right) + \left(\frac{z_o - z}{2\cos^2\bar{\theta}} \right) \bar{\theta}\sigma_\theta \ , \quad (2)$$

where σ_z is the standard deviation of the change in instrument depth, σ_θ is the standard deviation of the beam angle, and $\bar{\theta}$ = 0 is the mean beam angle for the vertical beam. The first term corrects for heaving of the beam and the second term corrects for its tilting. Using a typical value of σ_z = *0.01 m* and σ_θ = *0.01 rad* (~1°), Δr ~ *0.01 m*. Thus, the minimum value of r used for constructing the structure function was 0.1 m, i.e. an order of

magnitude larger that Δr. The maximum value of r was dictated by the proximity of the depth to the bed. Taylor's cascade theory relates the length scale, r and the rate of dissipation of turbulent kinetic energy with the characteristic length and velocity scales such as that for isotropic turbulent eddies:

$$D(z,r) = C_v^2 \varepsilon^{2/3} r^{2/3} \quad (3)$$

This relationship holds for values of r in the inertia sub-range bounded by the Kolmogorov microscale in the lower limit and the distance to the bed, in the absence of stratification, or Ozmidov scale in stratified flow in the upper limit. In order to estimate the dissipation rate, $D(z,r)$ is fitted to an equation:

$$D(z,r) = Ar^{2/3} + N\,, \quad (4)$$

where $A = C_v^2 \varepsilon^{2/3}$. Following [8] C_v = 2.1 from radar meteorology and is used in marine environments [10, 11]. N is an offset that includes the uncertainty due to inherent instrument noise and other non-turbulence related fluctuations. A least square fitting in the form of Equation 4 is used to estimate A and N, hence ε is obtained. Estimates are not made for heights with depth resulting in $D(z,r)$ less than 10 points. Within the valid depth, results of the fittings were quality controlled to remove estimates of ε with $R^2 < 0.6$. This resulted in loss of 23% and 25% data for the spring and neap results presented here, respectively.

Results and discussions

Presentation

Using the water level obtained from the Aquadopp profiler, we extracted dominant tidal constituents for the location. Coupled with the harmonic analysis of the current speed and direction, a robust prediction of the current within the vicinity of the ship is being developed. We summarise the basic results here. Figure 3 shows the power spectral densities (PSD) of the water level using the 53-days' observations. The spectra indicated strong amplitudes of diurnal, semi-diurnal, ter-diurnal and overtide tidal constituents. In addition, we observed a seiche wave with a period of 1.3 hours corresponding to the wave sloshing between the field location and the southern mainlands (Figure 1). Further analysis of the water level showed that the channel was characterised by a form number, a ratio of the sums of major diurnal and semi-diurnal constituents, of 0.28. Thus, the site can be considered a mixed tidal system with semi-diurnal dominance. The tidal range varied between 0.6 and 3.5 m such that the system is considered a micro-tidal estuary during the neap tides, and a meso-tidal estuary during the spring tides. Therefore, the subsequent results are focused on the comparisons between turbulent characteristics of the spring and neap tidal types.

Basic flow observation

The instantaneous velocities showed substantial fluctuations. The horizontal mean velocity is presented with positive indicating the ebb and negative indicating the flood flows. Similar to the water level, the horizontal velocities contained superimposition of fluctuations occurring at many different periods. Figure 4 shows mean near-bed horizontal velocity profiles for typical spring and ebb periods (separated by 7 days). In general, the spring tidal mean velocity amplitudes of about 0.6 m/s at about 6 m above the seabed were up to two times larger than those of the neap tide. On average, the magnitude of the flood tide was larger than the ebb, indicating an ebb-flood tidal asymmetry. This is likely associated with large shallow areas nearshore in the upstream, resulting in significant evaporation with relatively small freshwater input. The funnel-like shape and reduction in the cross-sectional area of the channel southwards possibly had a significant contribution to this ebb-flood asymmetry of the site.

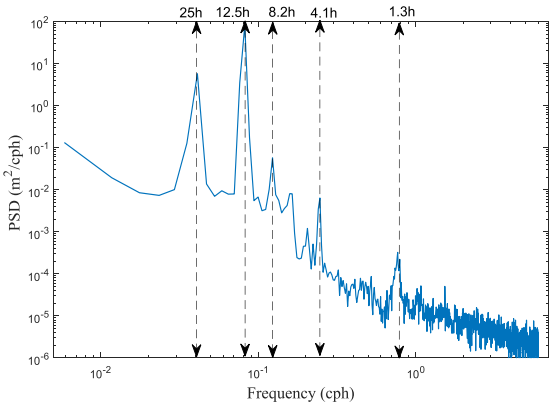

Figure 3. Power spectra density of the water level

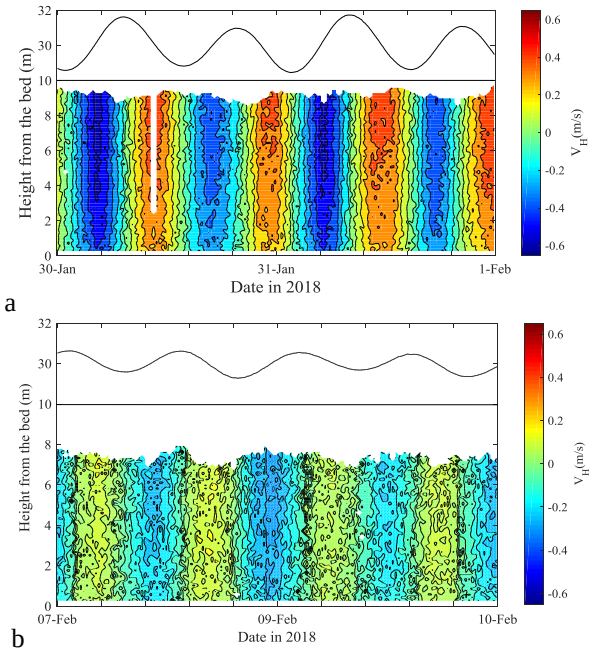

Figure 4. Mean horizontal velocities for 48-hour period showing typical (a) Spring tide, (b) Neap tide: Estimate made using a temporal averaging window of 20 minutes. Upper panels show the water level.

Spring-neap tides dissipation rates

Figure 5 shows the estimates of TKE dissipation rate between 0.3 and 2.1 m above the bed for the spring and neap tidal types. These estimates are made using a temporal window of 10 minutes obtained from sensitivity analysis. Consistent with the turbulent bottom boundary layer, the highest dissipation rates were found near the bed. The time series of ε showed a discernible semi-diurnal trend, with lower values occurring around the slack water and higher values occurring during the peak flows. The TKE dissipation rate ranges between 10^{-8} and 10^{-2} m^2/s^3 for the range of depth measured. For comparison, for a high flow tidal channel, ε ~ 10^{-5} - 10^{-4} m^2/s^3 were estimated, in The Bay of Fundy, Canada, where velocity amplitude was greater than 2 m/s [6], while ε varied between 10^{-4}-10^{-1} m^2/s^3 in Red Wharf Bay in the UK, where velocity amplitude was around 1 m/s [11]. On the lower end, estimates of ε~10^{-11} – 10^{-8} m^2/s^3 using the spectral method were made in a lake driven by wind and buoyancy with velocity amplitude limited to 0.03 m/s [3]. The rate of dissipation varied by up to four orders of magnitude over a tidal cycle ranging from 10^{-6} and 10^{-2} m^2/s^3 for the spring tide, while the neap tide ranged

between 10^{-8} and 10^{-5} m^2/s^3. This result indicated that the spring tides were more energetic than the neap, consistent with the tidal velocity amplitude. This suggests mixing near the bed was strongly tidally driven.

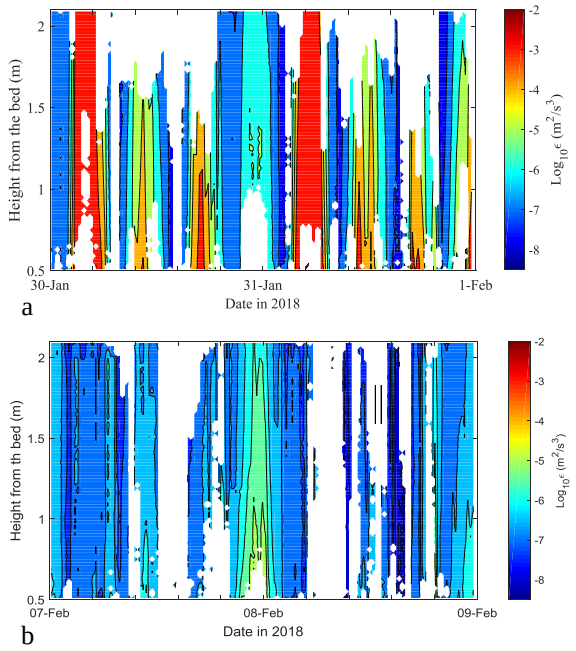

Figure 5. TKE dissipation rate (ε) for (a) Spring tide, (b) Neap tide: The white gaps indicate no or unreliable estimates removed through quality control as discussed in the text.

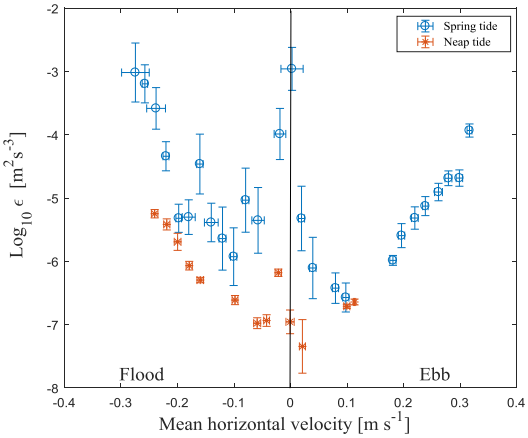

Figure 6. TKE dissipation rate (ε) binned by mean velocity; Error bars indicate the 95% confidence interval around mean values.

The vertical profiles of ε show that the turbulence level in the depth range observed was significantly higher on the flood tide compared to the ebb for both spring and neap tides. To further compare the rate of dissipation between the flood and the ebb tides, the estimated ε are averaged by bins of mean flow velocity with a bin size of 0.02 m/s using all valid depths (Figure 6). The variability is shown with error bars which indicate the 95% confidence interval around mean values. The result showed that for a specific flow speed, the spring tide was an order of magnitude more dissipative than the neap tide. Except around slack with mean speed less than 0.1 m/s where the scaling failed, ε is scaled as a power law with the mean speed u^{γ}, where power γ varied from 3 – 5. This is consistent with the boundary layer turbulence at mean depth below the water surface where $\varepsilon \sim |u|^3$, where production balances the dissipation of kinetic energy [7]. Further analysis will be carried out to examine the energy budget within the channel.

Summary and conclusion

Flow field data were sampled continuously at high frequency (4 Hz) from the mid-depth to the bottom boundary layer of an inverse estuary over 53 days. The water level and flow velocity showed substantial fluctuations during the observation period. The tidal range within the system varied such that the channel can be considered a micro-tidal and meso-tidal estuary during the neap and spring tides, respectively. We used the profile beam velocity of the vertical beam operated in high resolution configuration to examine the turbulence structure. In order to evaluate the energy budget within the channel, we performed a preliminary estimate of the rate of dissipation of turbulent kinetic energy, ε, within the lower 2m of the water column. In summary, the rate of dissipation of TKE showed a variation of up to four orders of magnitude within a tidal cycle, ranging between 10^{-6} and 10^{-2} m^2/s^3 for the spring, and between 10^{-8} and 10^{-5} m^2/s^3 for the neap tides. The variation of ε showed a clear semi-diurnal tidal pattern with flood-ebb asymmetry in relation to the mean flow. These datasets are under further analysis and will be used to provide quantitative information for managing the location including prediction of currents for diver experience and examining sediment transport and organic growths around Ex-HMAS Tobruk, scuttled in the site.

References

[1] Goring, D.G. and Nikora, V.I., *Despiking acoustic Doppler velocimeter data.* Journal of Hydraulic Engineering, 2002. **128**(1): p. 117-126. doi:10.1061/(ASCE)0733-9429(2002)128:1(117).

[2] Gräwe, U. (2009). *Hervey Bay-insights from numerical modelling into the hydrodynamics of an Australian subtropical bay*. PhD Thesis, Universität Oldenburg.

[3] Lorke, A. and Wüest, A., *Application of Coherent ADCP for Turbulence Measurements in the Bottom Boundary Layer*. Journal of Atmospheric and Oceanic Technology, 2005. **22**(11): p. 1821-1828. doi:10.1175/JTECH1813.1.

[4] Gräwe, U. (2009). *Hervey Bay-insights from numerical modelling into the hydrodynamics of an Australian subtropical bay*. PhD Thesis, Universität Oldenburg.

[5] Lucas, N.S., Simpson, J.H., Rippeth, T.P., and Old, C.P., *Measuring Turbulent Dissipation Using a Tethered ADCP*. Journal of Atmospheric and Oceanic Technology, 2014. **31**(8): p. 1826-1837.

[6] MacKinnon, J. and Gregg, M., *Mixing on the late-summer New England shelf—Solibores, shear, and stratification.* Journal of Physical Oceanography, 2003. **33**(7): p. 1476-1492.

[7] McMillan, J.M. and Hay, A.E., *Spectral and structure function estimates of turbulence dissipation rates in a high-flow tidal channel using broadband ADCPs.* Journal of Atmospheric and Oceanic Technology, 2017. **34**(1): p. 5-20.

[8] Sauvageot, H., *Radar meteorology*. 1992: Artech House Publishers.

[9] Suara, K.A., Brown, R.J., and Borgas, M., *Eddy diffusivity: a single dispersion analysis of high resolution drifters in a tidal shallow estuary.* Environmental Fluid Mechanics, 2016. **16**(5): p. 923 - 943. doi:10.1007/s10652-016-9458-z.

[10] Thomson, J., *Wave Breaking Dissipation Observed with "SWIFT" Drifters.* Journal of Atmospheric and Oceanic Technology, 2012. **29**(12): p. 1866-1882. doi:10.1175/JTECH-D-12-00018.1.

[11] Wiles, P.J., Rippeth, T.P., Simpson, J.H., and Hendricks, P.J., *A novel technique for measuring the rate of turbulent dissipation in the marine environment.* Geophysical Research Letters, 2006. **33**(21).